Desalination and Water Treatment
www.deswater.com
doi: 10.5004/dwt.2018.22409

114 (2018) 175–184
May

Thermal treatment of attapulgite for phosphate removal: a cheap and natural adsorbent with high adsorption capacity

Mun-Ju Kim[a], Jung-Hun Lee[a], Chang-Gu Lee[b], Seong-Jik Park[a,*]

[a]*Department of Bioresources and Rural System Engineering, Hankyong National University, Anseong, South Korea, Tel. +82 31 670 5131; emails: parkseongjik@hknu.ac.kr (S.-J. Park), kimmunju22@gmail.com (M.-J. Kim), sksdlwjdgns@naver.com (J.-H. Lee)*
[b]*Department of Environmental and Safety Engineering, Ajou University, Suwon, South Korea, Tel. +82 31 219 2405; email: changgu@ajou.ac.kr*

Received 18 November 2017; Accepted 20 April 2018

ABSTRACT

Attapulgite was used for the removal of phosphate in aqueous solution and was thermally treated to improve its phosphate adsorption capacity. Attapulgite treated at different temperatures was analyzed to characterize its physical and chemical properties and quantify its phosphate removal efficiency. Attapulgite treated at 700°C (700-ATP) was found to remove phosphate more efficiently than the attapulgite treated at the other temperatures did. The pseudo-second-order and Freundlich models were appropriate for describing phosphate adsorption onto 700-ATP for various reaction times and initial phosphate concentrations, respectively. Both enthalpy and entropy increased during phosphate adsorption onto 700-ATP. An increase in solution pH from 3 to 11 led to a decrease in the adsorption amount of phosphate from 51.53 to 42.43 mg/g. The influence of competitive anions on the phosphate adsorption was as follows: $HCO_3^- > SO_4^{2-} > NO_3^-$. Attempts to reutilize the 700-ATP with deionized water were not successful. Phosphorus fractionation experimentation showed that most of the phosphate in 700-ATP was present in residual form. Phosphorus was strongly adsorbed onto 700-ATP. This study demonstrated that thermal treatment is a simple but effective way to improve the phosphorus removal efficiency of attapulgite and 700-ATP is a low-cost, natural, and abundant material for the removal of phosphate from aqueous solution.

Keywords: Adsorption; Attapulgite; Batch experiment; Ca elution; P fractionation; Thermal treatment

1. Introduction

Phosphorus is a trigger of eutrophication in lakes because it is an additional nutrient for the growth of photosynthetic macroorganisms and microorganisms in aquatic water bodies [1]. Eutrophication of lakes leads to algal blooms and the depletion of dissolved oxygen at night [2]. To control eutrophication in natural waters, the removal of phosphorus from waters has been considered [3].

For the removal of phosphate from water, adsorption has been widely used because it does not require high cost, high energy, nor highly skilled operation [4]. The cost and efficiency of adsorption processes largely depend on the adsorbents. Natural minerals are good candidates for phosphate removal because of their low cost, ease of procurement, and less public concerns. Some industrial wastes, such as fly ash [5], red mud [6], steel slag [7,8], iron oxide tailings [9], and crushed concrete [10], have high phosphate adsorption capacities, but public concerns regarding their toxicity restrict their use for water treatment.

The application of natural minerals for water treatment has some advantages in terms of public concerns, cost, and environmental effects. Natural minerals are cheap when compared with synthetic materials, such as nanoadsorbents, layered double hydroxides, and other metal oxides.

* Corresponding author.

Extensive research has been carried out on the use of natural minerals as adsorbents. Alunite [11], calcite [12], dolomite [13], bentonite [14], boehmite [15], hydrocalumite [16], palygorskite [17], vesuvianite [18], and zeolite [19] have been used for phosphate removal. However, most of these natural minerals at untreated condition do not have high adsorption capacity for phosphate, and their adsorption capacities are usually less than 10 mg-P/g. Therefore, investigation is needed regarding the modification of natural minerals via coating with metals, such as Al, Fe, Zr, and La; acid treatment with HCl; and thermal treatment. Chemical modification does not lead to homogenous surface properties and generates chemical waste after modification processes. In addition to the issue of chemical waste production, there are public concerns regarding some of the chemicals used for the modification. Thermal treatment does not generate chemical waste and the surface of adsorbents can be easily modified with such treatment.

Attapulgite is a natural hydrous magnesium-aluminum silicate mineral, and its chemical formula is generally $Mg_5(Al)Si_8O_{20}(OH)_2(OH_2)_4{\cdot}4H_2O$ [20,21]. Attapulgite can be used as an adsorbent or a catalyst because of its unique pore channels, high surface area, and high adsorption capacity [22–24]. Compared with other minerals, the price of attapulgite is low. Iron oxide costs 900 US$/ton, and montmorillonite costs 300 US$/ton, whereas attapulgite has a price of 150 US$/ton. Some studies have shown that attapulgite is effective for phosphate removal from aqueous solutions [25–27]. However, more experimental study is required to improve our knowledge regarding the mechanism of phosphate adsorption onto attapulgite to apply it for phosphate removal in various environmental conditions.

In this study, we assessed the feasibility of attapulgite for the removal of phosphate in aqueous solution and thermally treated attapulgite to enhance its adsorption capacity for phosphate. The physical and chemical properties and adsorption amounts of attapulgite treated at different temperatures were investigated. Attapulgite treated at 700°C (700-ATP) was used for further investigation including in kinetic, isotherm, and thermodynamic studies. To determine the mechanism of phosphate adsorption onto 700-ATP, we also performed batch experiments at various pH values, with various attapulgite doses, and with other competitive anions present. Regeneration of 700-ATP was attempted using deionized water, and the phosphorus fraction in 700-ATP was investigated.

2. Materials and methods

2.1. Attapulgite preparation and characterization

The experiments were performed with natural attapulgite supplied by the Haihang Industry Co., China. The particle size of the attapulgite was <200 mesh (75 μm). The attapulgite was thermally treated using a tube furnace with a horizontal quartz glass tube (5.5 cm in diameter and 55 cm in length) at 100°C, 300°C, 500°C, 700°C, and 900°C (100-ATP, 300-ATP, 500-ATP, 700-ATP, and 900-ATP, respectively) for 4 h. Before thermal treatment, nitrogen gas was injected into the quartz glass tube to create anoxic conditions. All thermally treated attapulgite was stored in desiccators before use.

Several analyses were conducted to characterize the attapulgite treated at different temperatures (100-ATP, 300-ATP, 500-ATP, 700-ATP, and 900-ATP) and to investigate the mechanism of phosphate adsorption onto these attapulgites. A field emission scanning electron microscope (FE-SEM; S-4700, Hitachi, Japan) with an energy dispersive spectrometer (EDS) attached was used to investigate the surface morphology and elemental composition on the surface of the different attapulgites. The chemical composition of the attapulgites was also analyzed using an X-ray fluorescence spectrometer (XRF-1700, Shimadzu, Japan), and the mineralogical structures of the attapulgites were investigated via their patterns of X-ray diffraction (XRD; Rigaku Co., Japan). N_2 adsorption–desorption experiments were performed to measure the specific surface area of 100-ATP, 300-ATP, 500-ATP, 700-ATP, and 900-ATP using a surface area analyzer (Quadrasorb SI, Quantachrome Instrument, USA). From the N_2 adsorption–desorption isotherms, the specific surface area was determined via Brunauer–Emmett–Teller (BET) analysis. Elution experiments were performed to investigate the mechanism of phosphate removal by the different attapulgites. The results were obtained by measuring the concentration of cations present in the solution after 1 g of each adsorbent was reacted with 30 mL of deionized water. The concentrations of cations in the extracted solution were determined with an inductively coupled plasma optical emission spectrometer (Optima 8300, Perkin-Elmer, USA). A thermogravimetric analysis (TGA) with differential thermal analysis (DTA) were conducted to identify the mass change of attapulgite during thermal treatments using a thermogravimetric analyzer (TGA/DSC1/1600 LF, Thermo, Switzerland).

2.2. Adsorption experiment

To investigate the influence of temperature on the phosphate adsorption of attapulgite, 0.1 g of attapulgite treated at different temperatures was reacted with 30 mL of 100 mg/L phosphate solution in a 50 mL Falcon tube for 24 h. A standard 1,000 mg/L phosphate solution was prepared by mixing potassium hydrogen phosphate (K_2HPO_4) and potassium dihydrogen phosphate (KH_2PO_4), and then diluted and used for the experiment. After the adsorption reaction, the phosphate solution was separated from the adsorbent using filter paper (Cat no. 1822-047, Whatman, USA). The filtered sample was analyzed via the ascorbic acid method. The phosphate concentrations were measured at 880 nm in a UV/VIS spectrophotometer (Optizen POP QX, Mecasys, Korea). The 700-ATP material was found to be the most effective adsorbent for phosphate removal and thus was used in subsequent experiments. All batch experimental conditions were identical to those described earlier unless otherwise stated.

To investigate the fundamental characteristics of phosphate adsorption onto 700-ATP, kinetic, equilibrium, and thermodynamic adsorption experiments were performed under batch conditions. Furthermore, 700-ATP was also used in adsorption experiments in which the pH of the solution, the 700-ATP dose, and the mole concentration of competitive anions varied. The kinetic adsorption experiments were performed by reacting 0.1 g of 700-ATP with three different phosphate solutions, i.e., 10, 100, and 600 mg/L, and the phosphate solution was sampled at 0.25, 0.5, 1, 2, 3, 6, 12, and

24 h after reaction initiation. In the equilibrium adsorption experiments, the solution samples were collected and analyzed after 24 h reaction and the initial concentrations of the phosphate solutions were set at 5, 10, 50, 100, 200, 300, 500, 700, 1,000, and 2,000 mg/L. The thermodynamic adsorption experiments were performed by varying the reaction temperature to 15°C, 25°C, and 35°C. To investigate the influence of solution pH on phosphate adsorption, the pH of the phosphate solution was adjusted to 3, 5, 7, 9, and 11 using 0.1 M NaOH and 0.1 M HCl solutions. Phosphate adsorption using different doses (3.33, 6.67, 10.00, 13.33, and 16.67 g/L) of 700-ATP was also performed. The effect of the presence of competing anions on phosphate adsorption onto 700-ATP was studied using 1 and 10 mM of each Na_2SO_4, $NaHCO_3$, and $NaNO_3$ prepared in 300 mg/L of phosphate solution, respectively. All batch experiments were performed in triplicate.

The removal of phosphate by 700-ATP after regeneration was investigated. After the adsorption experiment with 1 g of 700-ATP and 30 mL of 300 mg/L phosphate solution, the separated 700-ATP was agitated in 30 mL of deionized water to desorb the phosphate from the 700-ATP. Additional adsorption tests were carried out using the same procedure described earlier. The adsorption experiment was repeated until the adsorption amount of 700-ATP was below 10 mg/g.

2.3. Fractionation experiment

The chemical compositional analysis of phosphorus distributed in attapulgite was based on the method suggested by Hieltjes and Lijklema [28]. Each fraction and its procurement method are as follows: (1) Total phosphorus (Tot-P): Add 20 mL of $HClO_4$ to 1 g of sample, boil for 2 h, add 100 mL of distilled water, adjust 5 mL of the solution to pH 1.8–2.2 using 5 N NaOH, and add another 50 mL of distilled water; (2) Adsorbed-P: Add 25 mL of 1 M NH_4Cl to 1 g of sample and shake for 2 h; (3) Nonapatite inorganic phosphorus (NAI-P): Add 25 mL of 0.1 N NaOH to 1 g of sample and shake for 17 h; (4) Apatite-P: Add 25 mL of 1 M HCl to 1 g of sample and shake for 24 h; and (5) Residual-P: Subtract Adsorbed-P, NAI-P, and Apatite-P from Tot-P.

2.4. Data analysis

The kinetic data can be analyzed using the following pseudo-first-order and pseudo-second-order models:

$$q_t = q_e\left(1-\exp\left(-k_1 t\right)\right) \tag{1}$$

$$q_t = \frac{k_2 q_e^2 t}{1+k_2 q_e t} \tag{2}$$

where q_t is the amount of phosphate removed at time t (mg-PO_4^{3-}/g), q_e is the amount of phosphate removed at equilibrium (mg-PO_4^{3-}/g), k_1 is the pseudo-first-order rate constant (h^{-1}), and k_2 is the pseudo-second-order velocity constant (g/mg-PO_4^{3-}/h).

The equilibrium data can be analyzed using the Langmuir (Eq. (3)), Freundlich (Eq. (4)), and Dubinin–Radushkevich (D-R) isotherm (Eq. (5)) models:

$$q_e = \frac{Q_m K_L C}{1+K_L C} \tag{3}$$

$$q_e = K_F C_e^{\frac{1}{n}} \tag{4}$$

$$q_e = Q_m \exp\left(\left(RT\ln\left(1+\frac{1}{C_e}\right)\right)^2 / -2E^2\right) \tag{5}$$

where C is the concentration of phosphate in the aqueous solution at equilibrium (mg-PO_4^{3-}/g), K_L is the Langmuir constant related to the binding energy (L/mg-PO_4^{3-}), Q_m is the maximum mass of phosphate removed per unit mass of attapulgite (removal capacity of attapulgite) (mg-PO_4^{3-}/g), K_F is the distribution coefficient (L/g), n is the Freundlich constant, R is the gas constant (8.314 J/K mol), and E is the adsorption energy (kJ/mol). Values of K_L, Q_m, K_F, and n can be determined by fitting the Langmuir and Freundlich models to the observed data.

The thermodynamic properties of the experimental results were analyzed using the following equations:

$$\Delta G^0 = \Delta H^0 - T\Delta S^0 \tag{6}$$

$$\Delta G^0 = -RT\ln K_e \tag{7}$$

$$\ln K_e = \Delta S^0 / R - \Delta H^0 / RT \tag{8}$$

$$K_e = \alpha q_e / C_e \tag{9}$$

where ΔG^0 is the change in Gibb's free energy, ΔS^0 is the change in entropy, ΔH^0 is the change in enthalpy, K_e is the equilibrium constant, and α is the amount of adsorbent.

3. Results and discussion

3.1. Characterization of attapulgite treated at different temperatures

Attapulgite treated at different temperatures was characterized via surface morphology, specific surface area, chemical composition, mineral structure, and ions eluted from different attapulgites. The characterization was performed in order to investigate the influence of such characteristics on the phosphate adsorption capacity of attapulgite treated at different temperatures. The surface morphologies of the attapulgites obtained using FE-SEM are shown in Fig. 1. Rod-like fibers that were present on the plate-like surface of nontreated attapulgite also appeared on the surface of 100-ATP and 300-ATP. However, as the temperature increased above 300°C, the number of the fibers began to disappear and were absent at 900°C. These results were consistent with those of specific surface area. As shown in Table 1, the specific surface area of attapulgite decreased from 85.5 to 48.6 m^2/g as the temperature increased from 100°C to 900°C. As the temperature increased from 700°C to 900°C in particular, a significant reduction in specific surface area was observed. The XRF data, as shown in Table 1, did not show significant changes in chemical composition of the attapulgites based on the temperature. The chemical composition obtained through EDS analysis also did not vary based on the temperature (Table S1). The chemical composition of the surface of the attapulgites was not sensitive to temperature, but the amount of cations eluted from the attapulgites

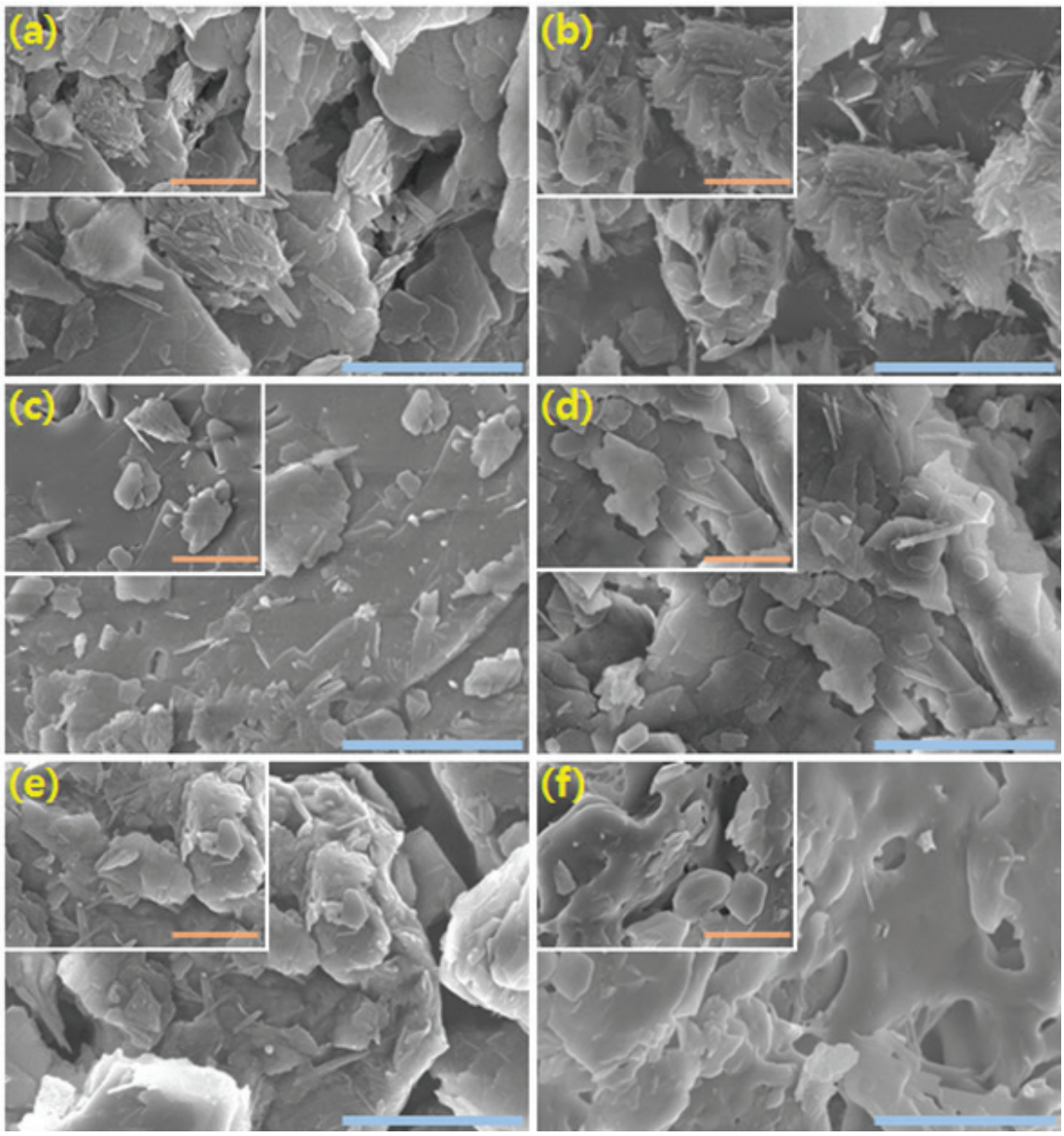

Fig. 1. SEM images of attapulgite treated at different temperatures: (a) untreated, (b) 100°C, (c) 300°C, (d) 500°C, (e) 700°C, and (f) 900°C (orange bar: 1 μm, blue bar: 2 μm). Quarter size figures on the upper-left corner end were acquired at an accelerating voltage of 15 kV and a magnification of ×40,000, and larger figures were obtained at an accelerating voltage of 5 kV and a magnification of ×20,000.

Table 1
BET specific surface area, XRF result, and amount of cation elution of attapulgite treated at different temperatures

Treatment	Surface area (m^2/g)	XRF result (%)								Elution result (mg/L)				
		SiO_2	Al_2O_3	MgO	CaO	Fe_2O_3	K_2O	SO_3	Others	Ca	K	Mg	Si	Al
Untreated	88.8	54.2	20.9	7.0	6.2	5.5	2.9	1.5	1.8	23.1	4.0	10.4	3.6	0.0
100°C	85.5	54.3	20.9	7.0	6.2	5.5	2.9	1.5	1.6	21.5	5.0	9.8	3.6	0.0
300°C	74.3	54.2	20.9	7.0	6.2	5.5	2.9	1.6	1.6	30.9	6.5	12.8	7.1	0.0
500°C	67.1	53.9	20.8	7.2	6.2	5.7	2.9	1.7	1.6	75.3	13.1	37.8	11.9	0.0
700°C	69.8	53.7	20.7	7.1	6.1	5.8	2.9	1.9	1.9	231.5	18.4	3.4	11.1	0.1
900°C	48.6	53.6	20.6	7.1	6.0	5.9	2.8	2.3	1.8	114.6	7.7	0.4	8.3	0.5

varied depending on the temperature. Compared with Ca concentration, the concentrations of Al and Fe eluted from the attapulgites were negligible. The concentrations of Ca eluted from the attapulgites were increased with increasing thermal temperature from 100°C to 700°C but that of 900-ATP was less than that of 700-ATP. Less Ca^{2+} elution from 900-ATP than 700-ATP can be explained by the formation of calcium-aluminum silicate above 700°C [25,29]. Lower intensity of XRD peaks of attapulgites was observed from the attapulgites treated at higher temperatures (Fig. S1). The higher concentrations of ions eluted from attapulgite at higher temperatures can be explained by the disruption of the crystalline structure of attapulgite at higher temperatures.

The phosphate adsorption on the attapulgites treated at different temperatures is shown in Fig. 2. Adsorbed phosphate on the untreated attapulgite was 0.7 mg/g, indicating nascent attapulgite is not useful for phosphate removal. The amounts of phosphate adsorbed onto 100-ATP, 300-ATP, and 500-ATP were 4.8, 4.6, and 3.9 mg/g, respectively, indicating a slight decrease in phosphate removal by attapulgite occurred as the temperature increased. Such a reduction of phosphate adsorption by higher thermally treated attapulgite can be explained by the decrease of specific surface area of attapulgite as the increase of thermal temperature on attapulgite.

As the temperature increased to 700°C, the phosphate adsorption increased sharply to 29.5 mg/g but the phosphate adsorption by 900-ATP was less than that by 700-ATP. The higher phosphate removal by 700-ATP than by the other attapulgites can be explained by the characteristics described earlier. It is well known that phosphate has a tendency to form chemical complexes with Al, Fe, and Ca metals. The calcium ions eluted from attapulgite can contribute to the formation of insoluble precipitates, such as $Ca_5(PO_4)_3OH$, $Ca_2HPO_4(OH)_2$, $CaHPO_4{\cdot}2H_2O$, and $Ca_3(HCO_3)_3PO_4$, with phosphorus [30–32]. As the highest amount of Ca was eluted from 700-ATP, the highest phosphate removal was observed for 700-ATP. Thus, further experiments were performed using 700-ATP. Similar observation of dye removal using attapulgite thermally treated at 700°C has been reported in other literatures [33,34].

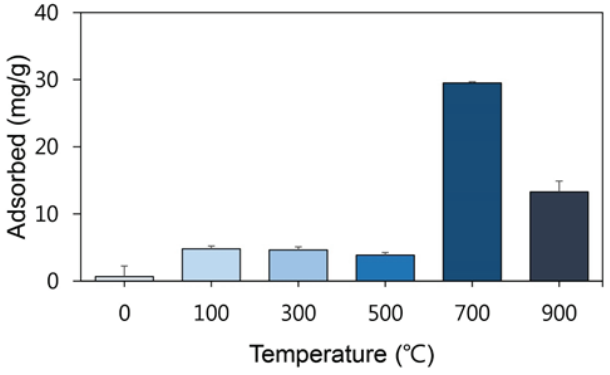

Fig. 2. Phosphate removal by attapulgite treated at different temperatures (initial phosphate concentration: 100 mg/L; pH: 7.0; attapulgite dosage: 3.33 g/L (0.1 g/30 mL); reaction time: 24 h; agitation speed: 100 rpm; temperature: 25°C).

TGA-DTA results also support the phosphorous removal using thermally treated attapulgite (Fig. S2). The first quick mass loss below 120°C was owing to the bound water removal of attapulgite sample, and the additional slow mass loss up to 500°C was related with removal of zeolitic water. The second sharp decline of mass from 500°C to 700°C was due to the dehydroxylation of Mg-OH groups in attapulgite [35]. This reaction caused the destruction of the attapulgite crystal, which leaded to an increase of specific surface area and adsorption capacity. Further thermal treatment caused a decrease in specific surface area and reduced the phosphate adsorption. The DTA curve showed the exothermic nature of attapulgite during thermal treatment.

3.2. Kinetic, isotherm, and thermodynamic studies

The phosphate adsorption onto 700-ATP as a function of reaction time at three different phosphate concentrations (10, 100, and 600 mg-PO_4^{3-}/L) is shown in Fig. 3. At a low initial concentration of phosphate (10 mg-PO_4^{3-}/L), phosphate adsorption reached equilibrium within 15 min. The time to reach equilibrium for 100 and 600 mg-PO_4^{3-}/L was 3 and 12 h, respectively, indicating that more time is required to reach equilibrium at higher concentrations of phosphate. As the initial phosphate concentration is increased, lower reaction constants k_1 and k_2 were obtained from both kinetic models, indicating that as the initial concentration increased, the sorption rate decreased (Table 2). Such a reduction of sorption rate at higher initial concentration of phosphate was also observed in other adsorbents including bentonite–alum and palm fibers [36,37]. At higher concentrations of phosphate, the pseudo-second-order model described the observed data obtained at different reaction times better than the pseudo-first-order model did, indicating that the adsorption rate of phosphate onto 700-ATP is controlled by chemisorption [38].

The relationship between the concentration of phosphate in aqueous phase and adsorbed phosphate onto 700-ATP at equilibrium is plotted in Fig. 4, and the parameters obtained from the Langmuir, Freundlich, and D-R models

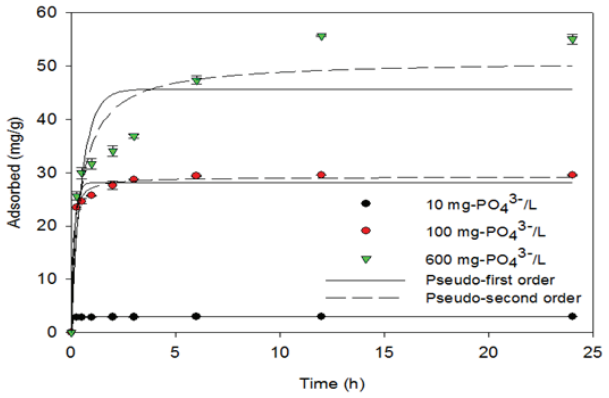

Fig. 3. Kinetic adsorption experiment data with model fittings of the pseudo-first-order and pseudo-second-order kinetic models for the adsorption of phosphate onto 700-ATP (initial phosphate concentration: 10, 100, and 600 mg/L; pH: 7.0; adsorbent dosage: 3.33 g/L; reaction time: 0.25, 0.5, 1, 2, 3, 6, 12, and 24 h; agitation speed: 100 rpm; temperature: 25°C).

Table 2
Kinetic model parameters obtained from model fitting of experimental data

Initial phosphate concentration (mg/L)	Pseudo-first-order kinetic model parameters			Pseudo-second-order kinetic model parameters		
	q_e (mg-PO_4^{3-}/g)	k_1 (h^{-1})	R^2	q_e (mg-PO_4^{3-}/g)	k_2 (g/mg/h)	R^2
10	14.9	19.89	0.999	15.0	31.84	0.999
100	28.2	6.30	0.974	29.2	0.45	0.993
600	45.7	1.92	0.785	51.0	0.04	0.890

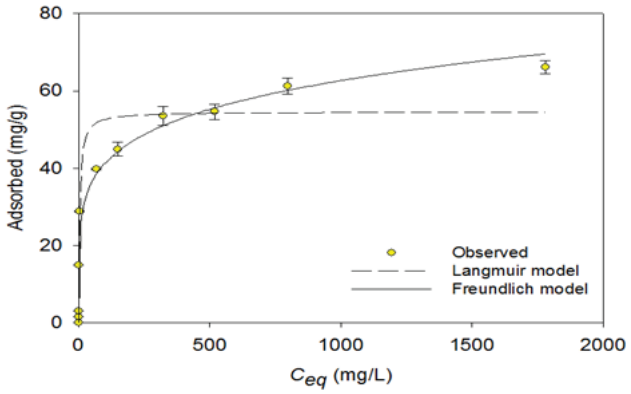

Fig. 4. Equilibrium adsorption experiment data with model fittings of the Freundlich and Langmuir isotherms for the adsorption of phosphate onto 700-ATP (initial phosphate concentration: 5, 10, 50, 100, 200, 300, 500, 700, 1,000, and 2,000 mg/L; pH: 7.0; adsorbent dosage: 3.33 g/L; reaction time: 24 h; agitation speed: 100 rpm; temperature: 25°C).

Table 3
Equilibrium model parameters obtained from model fitting of the experimental data

Model	Parameters		R^2
Langmuir	Q_m (mg-PO_4^{3-}/g) 54.4	K_L (L/mg) 3.71	0.910
Freundlich	K_F (L/g) 18.0	$1/n$ 0.18	0.969
D-R	Q_m (mg-PO_4^{3-}/g) 53.4	E (kJ/mol) 0.52	0.882

are shown in Table 3. The higher R^2 value of the Freundlich model (R^2 = 0.969) than of the Langmuir (R^2 = 0.910) and D-R (R^2 = 0.882) models indicates that phosphate adsorption onto 700-ATP occurred via multiple layer adsorption rather than monolayer adsorption. Fig. 4 also shows that the Freundlich model fits better to the observed data than the Langmuir and D-R models. The $1/n$ value of the Freundlich model was 0.18, which is less than 0.5, indicating that the binding between phosphate and 700-ATP was strong [39]. The maximum phosphate adsorption capacity of 700-ATP obtained from the Langmuir and D-R models were 54.4 and 53.4 mg/g, respectively. Adsorption energy (E) value from D-R model was 0.52 kJ/mol.

The maximum adsorption capacity of 700-ATP was comparable with that of other adsorbents published in the literature. Of the 39 adsorbents listed by Kang et al. [10], 28 had an adsorption capacity for phosphate that was less than the 54.4 mg/g achieved in the current study. Most of the adsorbents with higher adsorption capacity than 700-ATP were synthesized from Ta, Zr, La, and Li, which are very expensive metals. Nanoparticles also have high adsorption capacity for phosphate due to their high specific surface area, but the toxicity of nanoparticles restricts their use [40].

Phosphate adsorption onto 700-ATP based on the reaction temperature is shown in Fig. S3. The thermodynamic parameters obtained from the thermodynamic analysis using Eqs. (6)–(9) are provided in Table S2. As the temperature increased, the amount of phosphate adsorbed onto 700-ATP increased, as shown in Fig. S3. A positive ΔH^0 value in this study indicates that the phosphate adsorption onto 700-ATP was endothermic. The ΔS^0 value was 11.76 J/K mol, indicating that the level of disorder increased at the solid–liquid interface during the adsorption process. The ΔG^0 values decreased gradually with increasing temperature, with 5.85, 5.73, and 5.61 kJ/mol at 15°C, 25°C, and 35°C, respectively, which indicates that the involuntary of the adsorption reaction was enhanced by the rising temperature and phosphate adsorption at all temperatures in this study was nonspontaneous.

3.3. Effects of solution pH, attapulgite dosage, and competing anions

The effect of initial solution pH on the phosphate removal by 700-ATP is shown in Fig. 5(a). The highest phosphate adsorption onto 700-ATP appeared to be 51.5 mg/g at pH 3, and the amount of phosphate adsorbed decreased from 51.5 to 42.4 mg/g as the pH increased from 3.0 to 11.0, respectively. These results mirrored those in other studies, in which pH increase negatively affected phosphate removal by adsorbents such as palygorskite [29], sepiolite [41], and Zr/Al-pillared montmorillonite [42]. The phenomenon that phosphate adsorption is dependent on pH can be explained by the dissolution of cations from the adsorbent, surface charge of the adsorbent, and polyprotic nature of phosphate [29,41,43,44]. Higher pH values can decrease the amount of Mg^{2+}, Ca^{2+}, and Al^{3+} leaching from adsorbents [44], thus inhibiting phosphate removal by forming insoluble precipitates such as Ca-phosphate precipitates [45]. In addition, as the pH of the solution increased, the surface of the adsorbents became more negatively charged, thereby increasing the electrostatic repulsion between the phosphate ions and the negatively charged surface of the adsorbents. Considering the dissociation constants of phosphoric acid ($pK_{a,1}$ = 2.15, $pK_{a,2}$ = 7.20, $pK_{a,3}$ = 12.33), it can dissociate to form different

ionic species ($H_2PO_4^-$, HPO_4^{2-}, and PO_4^{3-}) depending on the pH of the solution [46]. When the pH ranges from 3 to 7, $H_2PO_4^-$ is the dominant form, but HPO_4^{2-}, a more negative ion, is the superior form in the solution when the pH ranges from 7 to 10.

The amount of phosphate adsorbed onto attapulgite and the removal percentages depending on the dose of 700-ATP are shown in Fig. 5(b). When the dose of 700-ATP increased from 0.1 to 0.5 g, the amount of phosphate adsorbed to unit mass of adsorbent decreased from 61.2 to 29.9 mg/g, but the percentage of phosphate removal increased from 20.4% to 49.8%. Similar to the equilibrium isotherm adsorption experiments, the increase in the ratio of adsorbate to adsorbent increased the amount of adsorbate per unit mass of adsorbent. By increasing the ratio of adsorbate to adsorbent, the concentration gradient between the aqueous phase and solid phase becomes larger, thereby increasing the driving force for adsorbate to the adsorbents [47].

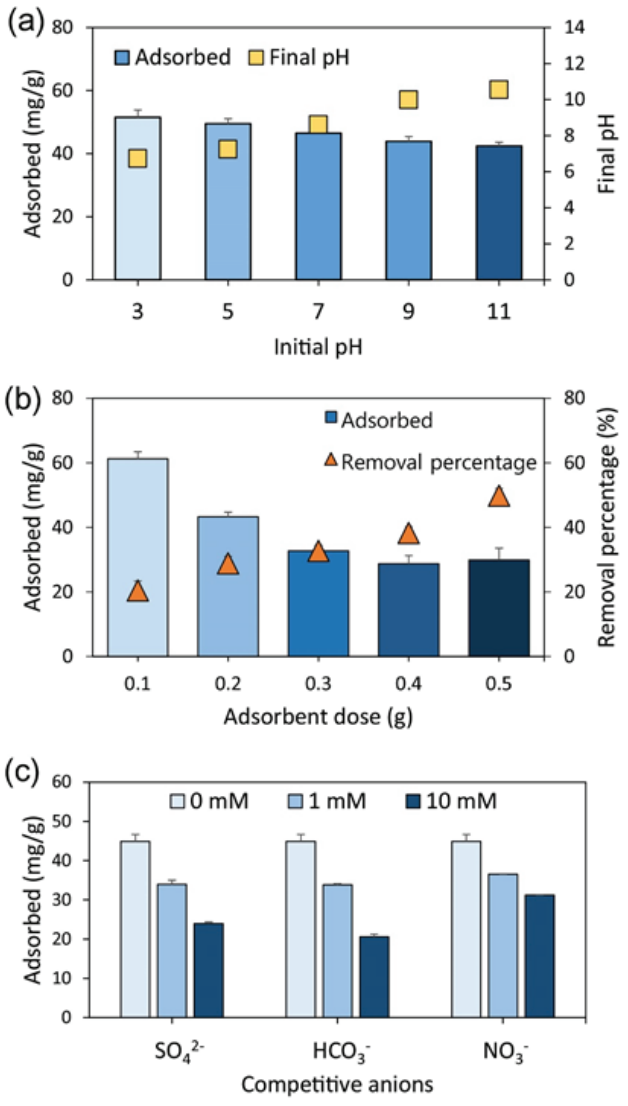

Fig. 5. Phosphate removal by 700-ATP under various environmental conditions: (a) solution pH, (b) dosage of 700-ATP, and (c) presence of competitive anions (SO_4^{2-}, HCO_3^-, NO_3^-) (initial concentration: 300 mg/L for solution pH and competitive anion experiments and 1,000 mg/L for dosage experiment; adsorbent dosage: 3.33 g/L; pH 7; reaction time: 24 h; agitation speed: 100 rpm; temperature: 25°C unless noted otherwise).

The influence of omnipresent aqueous anions including sulfate ions (SO_4^{2-}), bicarbonate ions (HCO_3^-), and nitrate ions (NO_3^-) on the phosphate adsorption by 700-ATP is presented in Fig. 5(c). The amounts of adsorbed phosphate in the presence of 1 mM of sulfate, bicarbonate, and nitrate were 33.9, 33.9, and 36.6 mg/g, respectively, indicating that the presence of such ions reduced the amount of phosphate adsorption but the differences were not significant. However, when the concentrations of sulfate, bicarbonate, and nitrate increased to 10 mM, the amounts of phosphate adsorption to unit mass of 700-ATP were 24.0 mg/g (SO_4^{2-}), 20.6 mg/g (HCO_3^-), and 31.2 mg/g (NO_3^-), respectively. The influence of nitrate on phosphate adsorption was less than that of the other two ions because nitrate can bind to metal via outer-sphere complexation in contrast to phosphate forming inner-sphere complexation with metal [48]. Even when the concentration of anions present was high, the amount of phosphate adsorption to 700-ATP was higher than 20 mg/g.

3.4. Reuse and P fraction of 700-ATP

Reutilization experiments were carried out to determine the amount of adsorbed phosphate and the number of times of use when 700-ATP was washed with distilled water. The amount of phosphate adsorption decreased from 45.0 to 8.1 mg/g as the number of times 700-ATP was reused increased, as shown in Fig. 6(a). According to these results, 700-ATP was not regenerated for phosphate removal by washing it with deionized water. Although better regeneration can be achieved via chemical regeneration using HCl and ethylenediaminetetraacetic acid or via electrical regeneration using a direct current power supply [49], these chemicals are too expensive to use for regenerating cheap adsorbents, i.e., 700-ATP. The regeneration experiments also indicated that phosphate was strongly adsorbed to 700-ATP by forming inner-sphere complexes, and the interaction between phosphate and 700-ATP was too strong for desorption.

Fig. 6(b) shows four different P fractions, i.e., adsorbed-P, NAI-P, apatite-P, and residual-P. The P fractionation results show that the phosphorus in 700-ATP was dominated by residual-P. The residual-P fractions in 700-ATP after reaction with 100 and 600 mg/L of phosphate were 96.5% and 95.6%, respectively. The other P fractions were negligible, with apatite-P as the second highest fraction, accounting for 2.4% and 3.5% at 100 and 600 mg/L of phosphate, respectively. The influence of initial phosphate concentration on P fractionation was not significant. The P fractionation results were consistent with those of the reutilization experiment, indicating that phosphate adsorbed on 700-ATP was too strongly bonded to be easily desorbed.

4. Conclusions

Attapulgite was used for phosphate removal, and thermal treatment of attapulgite was performed to improve its

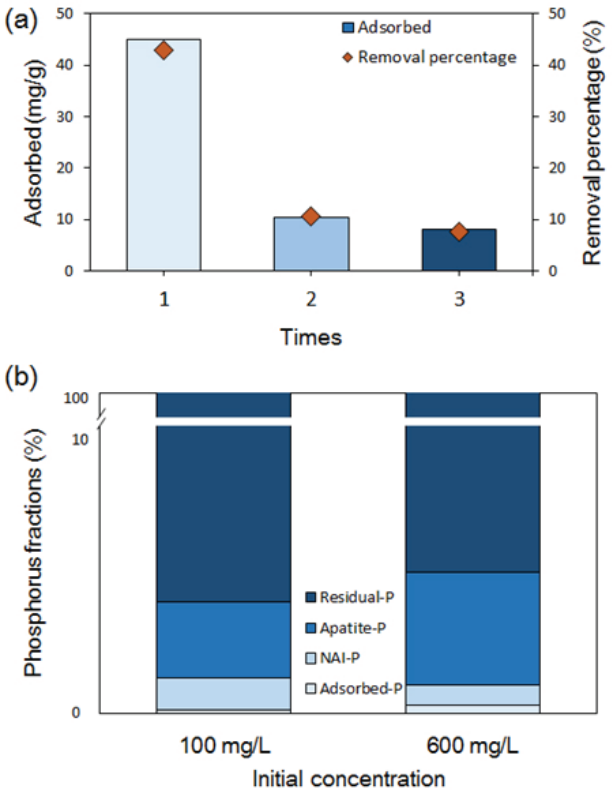

Fig. 6. (a) Amount of phosphate removal for increasing cycles of reutilization (initial phosphate concentration: 300 mg/L; pH: 7.0; reaction time: 24 h; agitation speed: 100 rpm; temperature: 25°C); (b) percentage of P fractions (initial phosphate concentration: 100, 600 mg/L; pH: 7.0; reaction time: 24 h; agitation speed: 100 rpm; temperature: 25°C).

adsorption capacity. Resultantly, 700-ATP removed more phosphate than the nontreated attapulgite and attapulgite treated at different temperatures did. The higher efficiency of 700-ATP was because more Ca ions were eluted from 700-ATP than from the other attapulgites. The kinetic study indicated that the rate of phosphate adsorption onto 700-ATP was limited mainly by chemisorption. The maximum adsorption capacity of 700-ATP obtained from Langmuir model fitting was 54.4 mg/g, which is comparable with that of other adsorbents reported in the literature. Phosphate adsorption onto 700-ATP was an endothermic reaction, with an increased level of disorder at the solid–liquid interface. Increasing the solution pH decreased phosphate adsorption owing to less dissolution of calcium ions from the adsorbent and larger electrostatic repulsion between phosphate ions and the surface of 700-ATP. Less influence of nitrate on phosphate removal by 700-ATP than of sulfate and carbonate was observed. Reutilization of 700-ATP and P fractionation experiments showed that phosphate was very strongly adsorbed onto 700-ATP. The results of the present investigation show that thermal treatment is an easy but effective way to improve the adsorption capacity of attapulgite. It can be concluded that thermally treated attapulgite can be used as a low-cost, natural, and abundantly available adsorbent for the removal of phosphate from aqueous solution.

Acknowledgment

This research was supported by Basic Science Research Program through the National Research Foundation of Korea (NRF) funded by the Ministry of Education (no. 2017R1D1A1B03030649).

References

[1] D.W. Schindler, Eutrophication and recovery in experimental lakes: implications for lake management, Science, 184 (1974) 897–899.
[2] E. Kurzbaum, Y. Raizner, O. Cohen, G. Rubinstein, O.B. Shalom, Lanthanum-modified bentonite: potential for efficient removal of phosphates from fishpond effluents, Environ. Sci. Pollut. Res., 24 (2017) 15182–15186.
[3] L. Ruixia, G. Jinlong, T. Hongxiao, Adsorption of fluoride, phosphate, and arsenate ions on a new type of ion exchange fiber, J. Colloid Interface Sci., 248 (2002) 268–274.
[4] J.H. Park, Y.S. Ok, S.H. Kim, J.S. Cho, J.S. Heo, R.D. Delaune, D.C. Seo, Evaluation of phosphorus adsorption capacity of sesame straw biochar on aqueous solution: influence of activation methods and pyrolysis temperatures, Environ. Geochem. Health, 37 (2015) 969–983.
[5] N.M. Agyei, C.A. Strydom, J.H. Potgieter, The removal of phosphate ions from aqueous solution by fly ash, slag, ordinary Portland cement and related blends, Cem. Concr. Res., 32 (2002) 1889–1897.
[6] S.G. Lu, S.Q. Bai, H.D. Shan, Mechanisms of phosphate removal from aqueous solution by blast furnace slag and steel furnace slag, J. Zhejiang Univ. Sci. A, 9 (2008) 125–132.
[7] Y. Li, C. Liu, Z. Luan, X. Peng, C. Zhu, Z. Chen, Z. Jia, Phosphate removal from aqueous solutions using raw and activated red mud and fly ash, J. Hazard. Mater., 137 (2006) 374–383.
[8] P. Castaldi, M. Silvetti, G. Garau, S. Deiana, Influence of the pH on the accumulation of phosphate by red mud (a bauxite ore processing waste), J. Hazard. Mater., 182 (2010) 266–272.
[9] L. Zeng, X. Li, J. Liu, Adsorptive removal of phosphate from aqueous solutions using iron oxide tailings, Water Res., 38 (2004) 1318–1326.
[10] K. Kang, C.G. Lee, J.W. Choi, S.G. Hong, S.J. Park, Application of thermally treated crushed concrete granules for the removal of phosphate: a cheap adsorbent with high adsorption capacity, Water, Air, Soil Pollut., 228 (2017) 8–16.
[11] M. Özacar, Adsorption of phosphate from aqueous solution onto alunite, Chemosphere, 51 (2003) 321–327.
[12] J.S. Freeman, D.L. Rowell, The adsorption and precipitation of phosphate onto calcite, Eur. J. Soil Sci., 32 (1981) 75–84.
[13] S. Karaca, A. Gürses, M. Ejder, M. Açıkyıldız, Kinetic modeling of liquid–phase adsorption of phosphate on dolomite, J. Colloids Interface Sci., 277 (2004) 257–263.
[14] M. Zamparas, A. Gianni, P. Stathi, Y. Deligiannakis, I. Zacharias, Removal of phosphate from natural waters using innovative modified bentonites, Appl. Clay Sci., 62 (2012) 101–106.
[15] F. Ogata, H. Tominaga, M. Kangawa, K. Inoue, N. Kawasaki, Characteristics of granular boehmite and its ability to adsorb phosphate from aqueous solution, Chem. Pharm. Bull., 60 (2012) 985–988.
[16] J.W. Son, J.H. Kim, J.K. Kang, S.B. Kim, J.A. Park, C.G. Lee, S.H. Lee, Analysis of phosphate removal from aqueous solutions by hydrocalumite, Desal. Wat. Treat., 57 (2016) 21476–21486.
[17] H. Ye, F. Chen, Y. Sheng, G. Sheng, J. Fu, Adsorption of phosphate from aqueous solution onto modified palygorskites, Sep. Purif. Technol., 50 (2006) 283–290.
[18] H. Li, J. Ru, W. Yin, X. Liu, J. Wang, W. Zhang, Removal of phosphate from polluted water by lanthanum doped vesuvianite, J. Hazard. Mater., 168 (2009) 326–330.
[19] S.L. Wang, H. Zhang, Z.J. Sun, L.S. Zheng, Treatment of phosphate-containing wastewater with zeolite, Mater. Protect. (China), 36 (2003) 55–56.

[20] Z. Wang, Y. Zhou, Y. Sun, Preparation, characterization and infrared emissivity study of attapulgite@ helical polyurethane composites, J. Inorg. Organomet. Polym. Mater., 19 (2009) 202–207.
[21] N.A. Azahari, N. Othman, H. Ismail, Effect of attapulgite clay on biodegradability and tensile properties of polyvinyl alcohol/corn starch blend film, Int. J. Polym. Mater., 61 (2012) 1065–1078.
[22] E. Cao, R. Bryant, D.J. Williams, Electrochemical properties of Na–attapulgite, J. Colloid Interface Sci., 179 (1996) 143–150.
[23] A. Li, A.Q. Wang, J.M. Chen, Preparation and properties of poly (acrylic acid-potassium acrylate)/attapulgite superabsorbent composite, J. Funct. Polym., 17 (2004) 200–206.
[24] J.M. Xu, W. Li, Q.F. Yin, Y.L. Zhu, Direct electrochemistry of Cytochrome c on natural nano-attapulgite clay modified electrode and its electrocatalytic reduction for H_2O_2, Electrochim. Acta, 52 (2007) 3601–3606.
[25] H. Yin, M. Kong, Simultaneous removal of ammonium and phosphate from eutrophic waters using natural calcium-rich attapulgite-based versatile adsorbent, Desalination, 351 (2014) 128–137.
[26] H. Yin, M. Han, W. Tang, Phosphorus sorption and supply from eutrophic lake sediment amended with thermally-treated calcium-rich attapulgite and a safety evaluation, Chem. Eng. J., 285 (2016) 671–678.
[27] H. Yin, X. Yan, X. Gu, Evaluation of thermally-modified calcium-rich attapulgite as a low-cost substrate for rapid phosphorus removal in constructed wetlands, Water Res., 115 (2017) 329–338.
[28] A.H. Hieltjes, L. Lijklema, Fractionation of inorganic phosphates in calcareous sediments, J. Environ. Qual., 9 (1980) 405–407.
[29] F. Gan, J. Zhou, H. Wang, C. Du, X. Chen, Removal of phosphate from aqueous solution by thermally treated natural palygorskite, Water Res., 43 (2009) 2907–2915.
[30] N. Cassagne, M. Remaury, T. Gauquelin, A. Fabre, Forms and profile distribution of soil phosphorus in alpine Inceptisols and Spodosols (Pyrenees, France), Geoderma, 95 (2000) 161–172.
[31] U. Berg, T. Neumann, D. Donnert, R. Nüesch, D. Stüben, Sediment capping in eutrophic lakes – efficiency of undisturbed calcite barriers to immobilize phosphorus, Appl. Geochem., 19 (2004) 1759–1771.
[32] J.F. Peng, B.Z. Wang, Y.H. Song, P. Yuan, Z. Liu, Adsorption and release of phosphorus in the surface sediment of a wastewater stabilization pond, Ecol. Eng., 31 (2007) 92–97.
[33] H. Chen, J. Zhao, A. Zhong, Y. Jin, Removal capacity and adsorption mechanism of heat-treated palygorskite clay for methylene blue, Chem. Eng. J., 174 (2011) 143–150.
[34] H. Chen, A. Zhong, J. Wu, J. Zhao, H. Yan, Adsorption behaviors and mechanisms of methyl orange on heat-treated palygorskite clays, Ind. Eng. Chem. Res., 51 (2012) 14026–14036.
[35] L. Boudriche, R. Calvet, B. Hamdi, H. Balard, Surface properties evolution of attapulgite by IGC analysis as a function of thermal treatment, Colloids Surf., A, 399 (2012) 1–10.
[36] R. Riahi, S. Chaabane, B.B. Thayer, A kinetic modeling study of phosphate adsorption onto *Phoenix dactylifera* L. date palm fibers in batch mode, J. Saudi Chem. Soc., 21 (2017) S143–S152.
[37] H. Mahadevan, V.V. Dev, K.A. Krishnan, A. Abraham, O.C. Ershana, Optimization of retention of phosphate species onto a novel bentonite–alum adsorbent system, Environ. Technol. Innovation, 9 (2018) 1–15.
[38] E. Bulut, M. Özacar, İ.A. Şengil, Equilibrium and kinetic data and process design for adsorption of Congo Red onto bentonite, J. Hazard. Mater., 154 (2008) 613–622.
[39] R.S. Summers, D.R.U. Knappe, V.L. Snoeyink, Adsorption of Organic Compounds by Activated Carbon, J.K. Edzwald, Ed., Water Quality and Treatment: A Handbook on Drinking Water, 6th ed., McGraw-Hill, New York, 2011.
[40] O. Bondarenko, K. Juganson, A. Ivask, K. Kasemets, M. Mortimer, A. Kahru, Toxicity of Ag, CuO and ZnO nanoparticles to selected environmentally relevant test organisms and mammalian cells in vitro: a critical review, Arch. Toxicol., 87 (2013) 1181–1200.
[41] H. Yin, M. Kong, C. Fan, Batch investigations on P immobilization from wastewaters and sediment using natural calcium rich sepiolite as a reactive material, Water Res., 47 (2013) 4247–4258.
[42] W. Huang, J. Chen, F. He, J. Tang, D. Li, Y. Zhu, Y. Zhang, Effective phosphate adsorption by Zr/Al-pillared montmorillonite: insight into equilibrium, kinetics and thermodynamics, Appl. Clay Sci., 104 (2015) 252–260.
[43] W. Chouyyok, R.J. Wiacek, K. Pattamakomsan, T. Sangvanich, R.M. Grudzien, G.E. Fryxell, W. Yantasee, Phosphate removal by anion binding on functionalized nanoporous sorbents, Environ. Sci. Technol., 44 (2010) 3073.
[44] H. Yin, Y. Yun, Y. Zhang, C. Fan, Phosphate removal from wastewaters by a naturally occurring, calcium-rich sepiolite, J. Hazard. Mater., 198 (2011) 362–369.
[45] C. Barca, C. Gérente, D. Meyer, F. Chazarenc, Y. Andrès, Phosphate removal from synthetic and real wastewater using steel slags produced in Europe, Water Res., 46 (2012) 2376–2384.
[46] W.Y. Huang, D. Li, J. Yang, Z.Q. Liu, Y. Zhu, Q. Tao, Y.M. Zhang, One-pot synthesis of Fe (III)-coordinated diamino-functionalized mesoporous silica: effect of functionalization degrees on structures and phosphate adsorption, Microporous Mesoporous Mater., 170 (2013) 200–210.
[47] R. Han, D. Ding, Y. Xu, W. Zou, Y. Wang, Y. Li, L. Zou, Use of rice husk for the adsorption of congo red from aqueous solution in column mode, Bioresour. Technol., 99 (2008) 2938–2946.
[48] J. Lin, Y. Zhan, H. Wang, M. Chu, C. Wang, Y. He, X. Wang, Effect of calcium ion on phosphate adsorption onto hydrous zirconium oxide, Chem. Eng. J., 309 (2017) 118–129.
[49] C.G. Lee, J.W. Jeon, M.J. Hwang, K.H. Ahn, C. Park, J.W. Choi, S.H. Lee, Lead and copper removal from aqueous solutions using carbon foam derived from phenol resin, Chemosphere, 130 (2015) 59–65.

Supplementary

Table S1
EDS of attapulgite thermally treated at different temperature

Element	C (%)	O (%)	Si (%)	Al (%)	Fe (%)	Mg (%)	Others (%)
None treated	36.29	43.3	10.92	4.18	1.87	1.82	1.62
100°C	42.84	38.91	8.58	3.49	1.48	2.23	2.47
300°C	56.69	31.46	5.5	3.32	0.34	0.35	2.34
500°C	56.96	31.1	5.99	4.14	0.33	0.17	1.31
700°C	34.18	36.69	14.06	11.01	0.69	0.43	2.94
900°C	21.92	39.81	19.95	4.88	3.65	4.78	5.01

Table S2
Thermodynamic parameters for phosphate adsorption onto 700-ATP

Temperature (°C)	ΔH^0 (kJ/mol)	ΔS^0 (J/K mol)	ΔG^0 (kJ/mol)
15	9.24	11.76	5.85
25			5.73
35			5.61

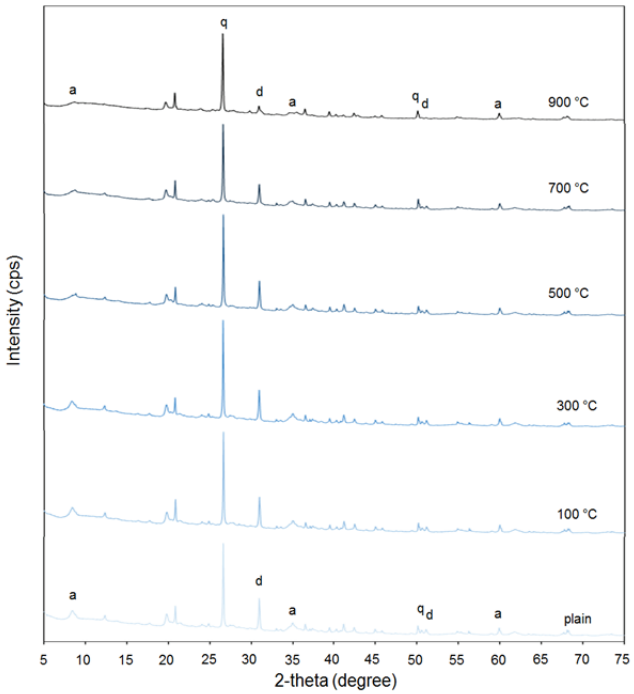

Fig. S1. XRD patterns of the attapulgite thermally treated at different temperature (none treated, 100°C, 300°C, 500°C, 700°C, 900°C): (a: attapulgite, d: dolomite, q: quartz).

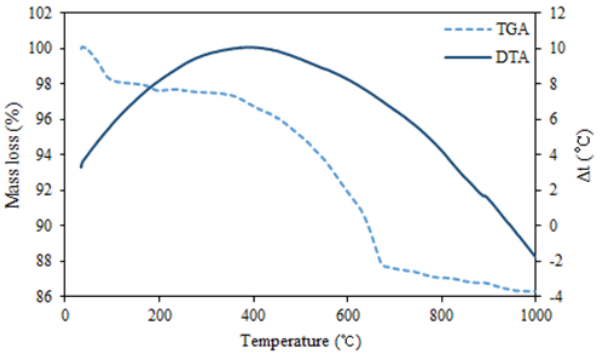

Fig. S2. Thermogravimetric analysis (TGA) and differential thermal analysis (DTA) curves of attapulgite depending on temperature.

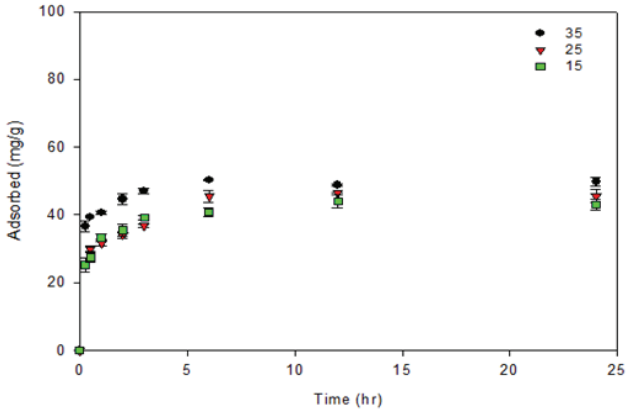

Fig. S3. Phosphate adsorption to 700-ATP as a function of reaction time under various temperatures (initial concentration: 300 mg/L; pH: 7.0; dosage amount: 0.1 g; reaction time: 15, 30 min, 1, 2, 3, 6, 12, 24 h; agitation speed: 100 rpm; temperature: 15°C, 25°C, 35°C).